

Magnetic transition in $\text{Er}_{1-x}\text{Y}_x\text{Co}_2$ ($x=0, 0.4$) single crystals probed by neutron scattering in magnetic fields

A. Podlesnyak,^{1,*} Th. Strässle,¹ J. Schefer,¹ A. Furrer,¹ A. Mirmelstein,² A. Pirogov,² P. Markin,^{2,3} and N. Baranov^{2,3}

¹Laboratory for Neutron Scattering, ETH Zürich and Paul Scherrer Institut, CH-5232 Villigen PSI, Switzerland

²Institute for Metal Physics RAS, 620219 Ekaterinburg GSP-170, Russia

³Institute of Physics and Applied Mathematics, Ural State University, 620083 Ekaterinburg, Russia

(Received 21 March 2002; published 16 July 2002)

Single-crystal neutron diffraction was employed to study the magnetic transition in the pseudobinary Laves-phase compounds $\text{Er}_{1-x}\text{Y}_x\text{Co}_2$ ($x=0, 0.4$) under external magnetic fields up to 4 T. The magnetic scattering amplitudes measured for the reflections to which either the localized $4f$ Er moment or the itinerant $3d$ Co moment solely contributes, give direct evidence that the onset of long-range magnetic order for both magnetic sublattices occurs at about the same temperature $T_C \sim 35.9$ and 17.0 K for $x=0$ and 0.4, respectively. The magnetic-susceptibility and specific-heat data, obtained on the same specimens, were also measured. In agreement with the neutron-diffraction data the macroscopic measurements showed no multiple phase transitions as opposed to earlier measurements on powder samples, which are presented and discussed as well.

DOI: 10.1103/PhysRevB.66.012409

PACS number(s): 75.30.Kz, 61.12.-q

The cubic pseudobinary Laves-phase compounds $R_{1-x}\text{Y}_x\text{Co}_2$ (R =rare-earth metal) are an important class of materials due to their complex magnetic properties provided by the intersublattice exchange field H_{fd} . Depending on the type of rare-earth element R and the yttrium concentration x they exhibit either exchange-enhanced paramagnetism, or continuous, or first-order (meta-)magnetic transitions (MT), associated with an itinerant electron metamagnetism (IEM) of the $3d$ electron Co subsystem.¹ Previously, bulk magnetic properties of $R_{1-x}\text{Y}_x\text{Co}_2$ were extensively studied by numerous research groups.²⁻⁶ Much attention was especially paid to the limited range around the critical concentration x_c at which H_{fd} becomes comparable to the critical field of the metamagnetic transition H_{cr} . Significant modifications of the temperature dependencies of the magnetovolume effect,²⁻⁴ electrical resistivity,^{2,4,5} magnetic susceptibility,⁶ and specific heat⁶ were observed in this case. A coexistence of short- and long-range magnetic order within a narrow concentration range near x_c was found by means of neutron powder diffraction.^{5,7} The magnetic state of compounds with $x > x_c$ was characterized as a spin glass.⁸

Despite the consensus on the general IEM features even some basic properties of the magnetic intersublattice interaction remain controversial. On one hand, in most previous studies one has assumed a common order transition temperature for both erbium and cobalt magnetic sublattices. On the other hand, detailed comparative measurements of the transport and magnetic properties of the ErCo_2 have shown that the resistivity drops at a temperature which is somewhat (~ 1 K) lower than T_C marked by the diverging susceptibility.⁹ This result has supposed that the onset of the cobalt magnetism appears at $T_0 \sim (T_C - 1)$ K. It has also been found in the $\text{Er}_{0.55}\text{Y}_{0.45}\text{Co}_2$ that the difference between the temperature at which magnetic neutron scattering disappears and the temperature of the sharp drop in resistivity attains ~ 6 K.⁵ However, authors concluded that different values of T_C obtained by different methods are caused by the inhomogeneous and complicated magnetic structure of the

compounds near x_c . Recently, it has been suggested that in $R_{1-x}\text{Y}_x\text{Co}_2$ in a limited concentration range around x_c a separate ordering of the two magnetic sublattices can be anticipated.^{10,11} The difference between the ordering temperatures of the itinerant cobalt and the rare-earth sublattices was proposed to depend strongly on x as well as on external pressure.¹¹⁻¹³ In particular, some anomalies observed on the temperature dependencies of the specific heat, thermal expansion, and electrical resistivity of polycrystalline $\text{Er}_{0.6}\text{Y}_{0.4}\text{Co}_2$ were ascribed to a double transition.¹⁰ The authors attribute the continuous phase transition at 14.5 K to magnetic ordering within the Er sublattice followed by a first-order transition at 11 K due to the metamagnetic behavior of the itinerant $3d$ sublattice.

Surprisingly, very little data on the magnetic behavior of $R_{1-x}\text{Y}_x\text{Co}_2$ by means of neutron-scattering methods have been published so far. In many cases the determination of the magnetization by neutron-diffraction techniques is invaluable in the interpretation of bulk phenomena, especially in the presence of several magnetic subsystems. Single-crystal measurements are highly desirable to diminish effects of chemical inhomogeneity and impurities.

In this paper we present results of neutron diffraction on single-crystal $\text{Er}_{1-x}\text{Y}_x\text{Co}_2$ with yttrium contents $x=0$ and 0.4 [i.e., just below the critical value $x_c \sim 0.45$ (Ref. 4)] which were undertaken to clarify the behavior of the magnetic erbium and cobalt subsystems near the critical concentration x_c . Furthermore, we present specific-heat and magnetic-susceptibility data of the very same specimens to compare T_C obtained by different methods.

The samples were prepared by arc melting under helium atmosphere followed by homogenization at 1220 K for 50 h. Single crystals (specimens of about $1 \times 1 \times 4$ mm³) were obtained by the Bridgman method. X-ray investigation of the samples revealed the cubic MgCu_2 structure type (space group $Fd\bar{3}m$) and cell parameters of $a=7.1568(5)$ Å ($x=0$) and $7.1826(5)$ Å ($x=0.4$) at ambient temperature in agreement with previous measurements for these compositions by others.³

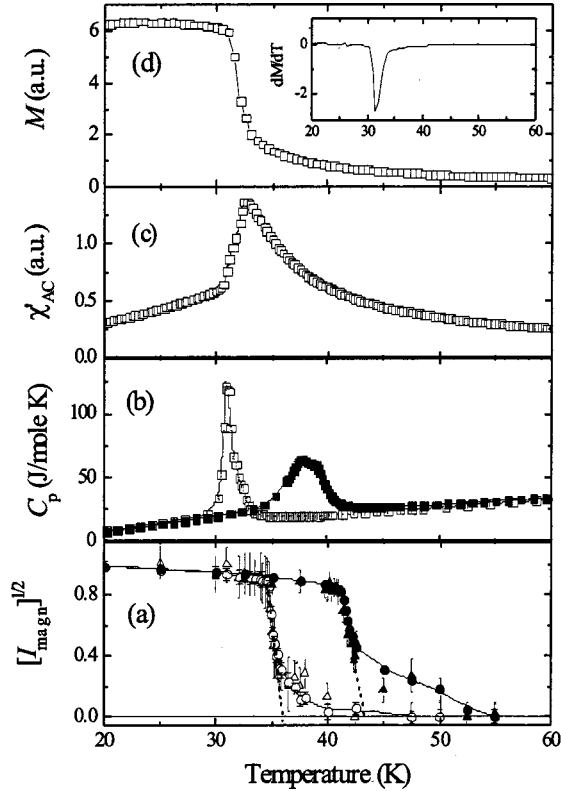


FIG. 1. Temperature dependence of (a) the square root of the normalized integrated intensities due to the (220) (circles) and (222) (triangles) magnetic Bragg reflections in ErCo_2 . Open and solid symbols represent data for an external magnetic field $\mu_0 H = 0$ and 4 T, respectively. The dashed lines are fits of the intensity drop with a straight line (see text). The solid lines are guides for the eye; (b) the specific heat $C_p(T)$ in 0 T (open boxes) and 4 T (filled boxes) applied field; (c) the real part of the ac susceptibility $\chi'_{ac}(T)$; (d) the field-cooled magnetization $M(T)$ at $\mu_0 H = 0.01$ T. The inset shows the dM/dT curve.

The neutron-diffraction studies were carried out on the TriCS four-circle diffractometer at the spallation source SINQ, Switzerland. The data were collected at a wavelength $\lambda = 1.179$ Å in a temperature range 4–55 K. An Oxford cryostat with a superconducting magnet was used for the measurements. A magnetic field up to 4 T was applied normal to the scattering plane and parallel to the [011] axis of the specimen. The heat-capacity and magnetic-susceptibility measurements were performed on a Quantum Design PPMS system. The ac susceptibility was measured at a frequency of 1 kHz and a field amplitude of 1×10^{-3} T.

Since the erbium and cobalt magnetic moments of $\text{Er}_{1-x}\text{Y}_x\text{Co}_2$ compounds have been well established earlier by magnetization measurements,^{6,14} NMR,¹⁴ and neutron diffraction,^{4,7,15} we chose to concentrate on the temperature behavior of the normalized intensities of several Bragg reflections. There are six different types of structure factors in the cubic MgCu_2 type, depending on the values of h , k , and l . It is important to stress that two of them are characteristic for the Er atoms only (h , or k , or $l \neq 4n$ and $h+k+l=4n$) or for the Co atoms only (h , k , and $l=4n+2$). Consequently, the square root of the normalized integrated magnetic inten-

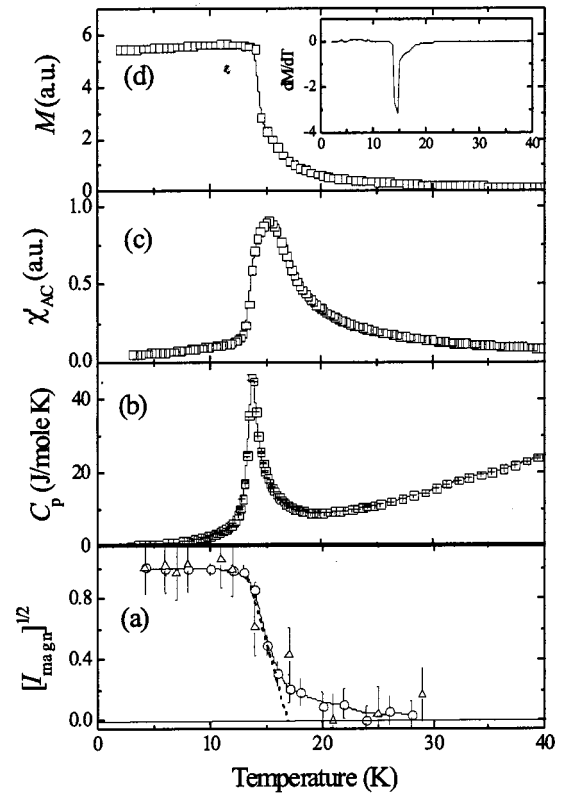


FIG. 2. Temperature dependence of (a) the square root of the normalized integrated intensities due to the (220) (circles) and (222) (triangles) magnetic Bragg reflections in $\text{Er}_{0.6}\text{Y}_{0.4}\text{Co}_2$. The dashed line is a fit of the intensity drop with a straight line (see text); the solid lines are guides for the eye; (b) the specific heat $C_p(T)$; (c) the real part of the ac susceptibility $\chi'_{ac}(T)$; (d) the field-cooled magnetization $M(T)$ at $\mu_0 H = 0.01$ T. The inset shows the dM/dT curve.

sities $I_{magn}^{1/2}(T) = \{[I(T) - I(60 \text{ K})] / [I(4 \text{ K}) - I(60 \text{ K})]\}^{1/2}$ for the (222) and (220) reflections directly monitor the magnetic moments μ_{Co} and μ_{Er} , respectively.

The analysis of the neutron-diffraction data of ErCo_2 [see Fig. 1(a)] and $\text{Er}_{0.6}\text{Y}_{0.4}\text{Co}_2$ [Fig. 2(a)] shows that at least two temperature intervals have to be considered in the vicinity of T_C : (i) In the temperature range $36 \leq T \leq 43$ K for ErCo_2 ($16 \leq T \leq 20$ K for $\text{Er}_{0.6}\text{Y}_{0.4}\text{Co}_2$), the integrated peak intensities essentially reveal the establishment of a magnetic order in the presence of strong spin fluctuations. The data obtained in external field shows even more pronounced fluctuation behavior. From Figs. 1 and 2(a) we deduce that magnetic intensity above T_C is observed for both (222) and (220) Bragg reflections, i.e., for both erbium and cobalt sublattices. Note that spin fluctuations have been shown to give dominant contributions to the IEM at finite temperature,^{16,17} in agreement with the present neutron-diffraction data. Key physical properties of the nonmagnetic $R\text{Co}_2$ ($R = \text{Sc}, \text{Y}, \text{Lu}$) compounds also have been inferred to be due to spin fluctuations,^{18,19} such as the enhanced linear term in $C_p(T)$ and the T^2 increase of the resistivity at low T followed by a saturation of ρ at ambient temperatures. A coexistence of short- and long-range magnetic order in diluted $R_{1-x}\text{Y}_x\text{Co}_2$

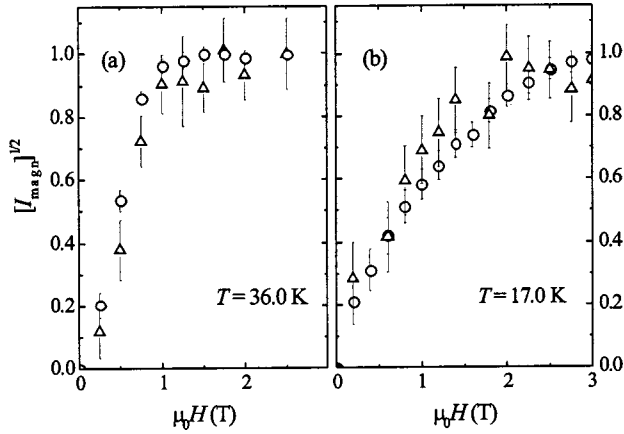


FIG. 3. Magnetic-field dependence of the square root of the normalized integrated intensities of the (220) (circles) and (222) (triangles) magnetic Bragg reflections in the (a) ErCo_2 and (b) $\text{Er}_{0.6}\text{Y}_{0.4}\text{Co}_2$, respectively.

was recently established by neutron diffraction on polycrystalline samples.^{5,7}

(ii) A simultaneous jump in relative intensity of both the (222) and the (220) magnetic Bragg reflections from ~ 0.25 to 0.85 of their maximal values takes place within $\Delta T = 0.9$ K for ErCo_2 ($\Delta T = 2.3$ K for $\text{Er}_{0.6}\text{Y}_{0.4}\text{Co}_2$), which clearly indicates that both Er and Co magnetic sublattices order at the same temperature. It should be noticed that the small (222) magnetic intensity in $\text{Er}_{0.6}\text{Y}_{0.4}\text{Co}_2$ does not allow determination of the temperature dependence of μ_{Co} with the same accuracy as for μ_{Er} . Nevertheless, within experimental uncertainty, we did not find any evidence for the decoupling of the magnetic ordering for the erbium and the cobalt sublattice. In this sense we have defined the ordering temperature T_C via the onset of long-range magnetic order determined by the intersection of the tangent at the inflection point and the zero line in Figs. 1 and 2(a).

The field-induced MT, as measured by neutron diffraction, is shown in Figs. 3(a) and 3(b) for the ErCo_2 and $\text{Er}_{0.6}\text{Y}_{0.4}\text{Co}_2$, respectively. From these data we also deduce that, within experimental uncertainty, the MT occurs simultaneously for both magnetic sublattices. An increased width of the transition in $\text{Er}_{0.6}\text{Y}_{0.4}\text{Co}_2$, as a function of both temperature and field, may be explained by a statistical distribution of yttrium and erbium atoms resulting in local magnetic inhomogeneities.

Macroscopic measurements carried out on the very same single-crystal samples are shown in panels Figs. 1(b)–1(d) and Figs. 2(b)–2(d). For both samples ($x=0,0.4$) provide evidence that multiple transitions are not found, neither in the heat-capacity nor in the dc magnetization and ac susceptibility measurements. Depending on the procedure used to define the magnetic transition temperature, different values for T_C may be obtained, though (see Table I). We note that the diverging C_p peak and the inflection point in the real part of the magnetic susceptibility are found at temperatures co-

TABLE I. Characteristic values of the magnetic transitions derived from the temperature dependencies of the square root of the normalized integrated intensities (T_C); maxima of the heat capacity (T_0^{HC}) and the real part of ac susceptibility (T_0^X); saturation of dc magnetization (T_0^M) and minimum of the dM/dT curve ($T_0^{dM/dT}$).

	ErCo_2	$\text{Er}_{0.6}\text{Y}_{0.4}\text{Co}_2$
T_C	35.9(5)	17.0(5)
T_0^{HC}	31.0(1)	13.8(1)
T_0^X	32.3(1)	15.2(1)
T_0^M	31.1(1)	14.0(1)
$T_0^{dM/dT}$	31.8(1)	14.5(1)

inciding with the saturation of the μ_{Co} and μ_{Er} moments as determined by the magnetization measurements (Figs. 1 and 2). The comparison of the absolute values of T_C derived by neutron diffraction and by means of macroscopic measurements needs to be done carefully since, with the cryostat used for the neutron-diffraction measurements, the exchange gas pressure may imply a difference between the true sample and the thermometer temperature. Apparently for this reason the value of T_C in ErCo_2 measured by neutron diffraction is found to be larger than that derived from the macroscopic measurements.

In summary, single-crystal neutron-diffraction experiments on $\text{Er}_{1-x}\text{Y}_x\text{Co}_2$ ($x=0, 0.4$) showed that both the Er and the Co magnetic sublattice order at the same temperature $T_C = 35.9(5)$ and $17.0(5)$ K, respectively. Our macroscopic measurements on single-crystal samples did not show two separate peaks neither for the specific heat, nor for the magnetic susceptibility, in disagreement with recently reported experiments on polycrystalline materials.^{10,20} The multiple magnetic transitions observed for polycrystalline samples could possibly be explained (i) by sample segregation into yttrium-rich and yttrium-poor regions resulting in different (local) transition temperatures, or (ii) by some $(R_{1-x}Y_x)_n\text{Co}_m$ impurities known to exhibit a variety of different magnetic structures and transition temperatures. Moreover, our neutron-diffraction data revealed magnetic scattering in a temperature region already above T_C due to short-range magnetic correlations and strong spin fluctuations. This result qualitatively supports a model for the magnetic state of these compounds in which the magnetization is associated to magnetic inhomogeneities (localized spin-density fluctuations).^{5,21}

We hope that our results contribute to a better understanding of the nature of the metamagnetic transition in itinerant electron systems and stimulate further neutron-scattering experiments under multiple (H, p) extreme conditions.

Financial support by the Swiss National Science Foundation (SCOPES Grant No. 7 IP 65598), the Russian State program “Neutron Investigation of Matter” [State Contract No. 107-19(00)-P-D01], and the Ministry of Education of the Russian Federation (Grant No. E00-3.4-259) is gratefully acknowledged.

- *Electronic address: andrew.podlesnyak@psi.ch Also at Institute for Metal Physics RAS, 620219 Ekaterinburg GSP-170, Russia.
- ¹For a review, see, for example, R.Z. Levitin and A.S. Markosyan, *Usp. Fiz. Nauk.* **155**, 623 (1988) [*Sov. Phys. Usp.* **31**, 730 (1988)]; J. J. M. Franse and R. Radwanski, in *Handbook of Magnetic Materials*, edited by K. H. J. Buschow (Elsevier Science Publishers B. V., North-Holland, Amsterdam, 1993) Vol. 7, Chap. 5, p. 730.
- ²W. Steiner, E. Gratz, H. Ortbauer, and H.W. Camen, *J. Phys. F: Met. Phys.* **8**, 1525 (1978).
- ³R.Z. Levitin, A.S. Markosyan, and V.V. Snegirev, *Phys. Met. Metallogr.* **57**, 56 (1984).
- ⁴N.V. Baranov, A.I. Kozlov, A.N. Pirogov, and E.V. Sinitsyn, *Zh. Eksp. Teor. Fiz.* **96**, 674 (1989) [*Sov. Phys. JETP* **69**, 382 (1989)].
- ⁵N.V. Baranov and A.N. Pirogov, *J. Alloys Compd.* **217**, 31 (1995).
- ⁶N.H. Duc, T.D. Hien, P.E. Brommer, and J.J.M. Franse, *J. Phys. F: Met. Phys.* **18**, 275 (1988).
- ⁷A. Podlesnyak, T. Strässle, A. Mirmelstein, A. Pirogov, and R. Sadykov, *Eur. Phys. J. B* (to be published).
- ⁸R. Kuentzler and A. Tari, *J. Magn. Magn. Mater.* **61**, 29 (1986).
- ⁹T.D. Cuong, L. Havela, V. Sechovsky, A.V. Andreev, Z. Arnold, J. Kamarad, and N.H. Duc, *J. Appl. Phys.* **81**, 4221 (1997).
- ¹⁰R. Hauser, E. Bauer, E. Gratz, M. Rotter, G. Hilscher, H. Michor, and A.S. Markosyan, *Physica B* **237/238**, 577 (1997).
- ¹¹R. Hauser, C. Kussbach, R. Grössinger, G. Hilscher, Z. Arnold, J. Kamarad, A.S. Markosyan, E. Chappel, and G. Chouteau, *Physica B* **294/295**, 182 (2001).
- ¹²A.S. Markosyan, R. Hauser, M. Galli, E. Bauer, E. Gratz, G. Hilscher, K. Kamishima, and T. Goto, *J. Magn. Magn. Mater.* **185**, 235 (1998).
- ¹³R. Hauser, E. Bauer, E. Gratz, H. Muller, M. Rotter, H. Michor, G. Hilscher, A.S. Markosyan, K. Kamishima, and T. Goto, *Phys. Rev. B* **61**, 1198 (2000).
- ¹⁴R.M. Moon, W.C. Koehler, and J. Farell, *J. Appl. Phys.* **36**, 978 (1965).
- ¹⁵A. Pirogov, A. Podlesnyak, T. Strässle, A. Mirmelstein, A. Teplykh, D. Morozov, and A. Yermakov, *Appl. Phys. A* (to be published).
- ¹⁶D. Wagner, *J. Phys.: Condens. Matter* **1**, 4635 (1989).
- ¹⁷H. Yamada, *J. Magn. Magn. Mater.* **139**, 162 (1995).
- ¹⁸N. Baranov, E. Bauer, E. Gratz, R. Hauser, A. Markosyan, and R. Resel, in *Physics of Transition Metals*, edited by P. M. Oppeneer and J. Kubler (World Scientific, Singapore, 1993), Vol. 1, p. 370.
- ¹⁹E. Gratz, N. Bernhoeft, V. Paul-Boncour, H. Casalta, and A. Murani, *J. Phys.: Condens. Matter* **12**, 5507 (2000).
- ²⁰A. Giguere, M. Foldeaki, W. Schnelle, and E. Gmelin, *J. Phys.: Condens. Matter* **11**, 6969 (1999).
- ²¹N.V. Baranov, A.A. Yermakov, A.N. Pirogov, A.E. Teplykh, K. Inoue, and Y. Hosokoshi, *Physica B* **269**, 284 (1999).